



HAL
open science

Envirotyping to Drive Spring Barley Adaptation in Northwestern Europe

Maëva Bicard, Michel-Pierre Faucon, Christoph Dockter, Dominique Vequaud, Pierre A. Pin, Renaud Rincenc, Chloé Elmerich, Bastien Lange

► **To cite this version:**

Maëva Bicard, Michel-Pierre Faucon, Christoph Dockter, Dominique Vequaud, Pierre A. Pin, et al.. Envirotyping to Drive Spring Barley Adaptation in Northwestern Europe. *Field Crops Research*, 2025, 326, pp.109793. <10.1016/j.fcr.2025.109793>. <hal-04997035>

HAL Id: hal-04997035

<https://normandie-univ.hal.science/hal-04997035v1>

Submitted on 19 Mar 2025

HAL is a multi-disciplinary open access archive for the deposit and dissemination of scientific research documents, whether they are published or not. The documents may come from teaching and research institutions in France or abroad, or from public or private research centers.

L'archive ouverte pluridisciplinaire **HAL**, est destinée au dépôt et à la diffusion de documents scientifiques de niveau recherche, publiés ou non, émanant des établissements d'enseignement et de recherche français ou étrangers, des laboratoires publics ou privés.



HAL Authorization

1 **Envirotyping to Drive Spring Barley Adaptation in Northwestern Europe**

2
3 Maëva BICARD^{a,b,*}, Michel-Pierre FAUCON^a, Christoph DOCKTER^c, Dominique VEQUAUD^d,

4 Pierre PIN^d, Renaud RINCENT^e, Chloé ELMERICH^a, Bastien LANGE^{a*}

5 ^aUniLaSalle, AGHYLE, Beauvais, France

6 ^bKronenbourg, Obernai, France

7 ^cCarlsberg Research Laboratory, Copenhagen, Denmark

8 ^dSecobra Recherches, Maule, France

9 ^eUniversité Paris-Saclay, INRAE, CNRS, AgroParisTech, GQE - Le Moulon, Gif- sur- Yvette,
10 France

11 *Corresponding author: maeva.bicard@unilasalle.fr (M. Bicard); bastien.lange@unilasalle.fr (B.

12 Lange)
13

14

15

16 **Abstract**

17 *Context:* Cereal crops are highly vulnerable to extreme climatic events. Due to the restricted genetic
18 diversity within the existing elite germplasm used in modern breeding, developing high-yielding and
19 stable cultivars in the context of climate change requires deciphering genotype x environment
20 interactions (GEI), commonly observed in multi-environment trials (METs).

21 *Objectives:* Our study on two-row spring barley, an economically important short-cycle crop, aimed to
22 (i) highlight the main environmental covariates (EC) – climatic variables calculated over phenological
23 stages – driving GEI for yield, and (ii) characterize genotypes' adaptation across the European spring
24 malting barley production area.

25 *Methods:* Using data from 112 elite genotypes across 121 environments (from 2015 to 2022), 91 EC
26 were calculated for each environment using the calibrated CERES-Barley model and analyzed for
27 their contribution to GEI. An environmental classification was conducted on the main GEI-drivers
28 across 1450 environments, including tested and untested locations, within the production area.

29 *Results:* Elevated temperatures during barley stem elongation, as well as solar radiation intensity and
30 water accessibility during grain filling, were identified as the major GEI-drivers. Thermal amplitude
31 around anthesis also emerged as an influential factor. The analysis discriminated three environment
32 types (ET) across the European Target Population of Environments (TPE), distributed according to
33 clear spatial and repeatability variations. They contrasted mainly in terms of temperatures during
34 vegetative growth, solar radiation intensity, and water availability during grain filling. Specific (suited
35 to one ET) or broad adaptation (multi-ET) were identified for the tested genotypes, offering valuable
36 information for characterizing germplasm performance and optimizing selection criteria.

37 *Conclusion:* We showed how controlling GEI-drivers through envirotyping enhanced year-to-year
38 field trial predictability, selection intensity, and yield genetic gain and stability. Further advancements
39 will need to integrate the genetic sensitivity to GEI-drivers into genomic selection methods to improve
40 accuracy in modern cereal breeding.

42 **Keywords**

43 Barley, Crop modeling, Ecophysiology, Genotype x environment interactions, Plant breeding, Target

44 population of environments

45

46

47 1. Introduction

48

49 Adapting crops to the climate and climate instability is crucial to ensure food security. Global surface
50 temperatures from 2011 to 2020 were 1.09°C higher than in 1850–1900, and this warming has
51 accelerated over the past two decades (IPCC, 2023). Extreme weather events, associated with year-to-
52 year climatic variability, are challenging the production stability and quality of major crops, including
53 cereals (Trnka et al., 2014; Webber et al., 2018; Xie et al., 2018; Vogel et al., 2019). Breeding efforts
54 are being made to develop stable cultivars that outperform the existing germplasm under evolving
55 biotic and abiotic stress conditions (Touzy et al., 2019; Snowden, 2021; Raina et al., 2022; Cooper et
56 al., 2023). However, genetic gain can be strongly compromised by genotype x environment
57 interactions (GEI) effects observed in multi-environment trials (MET), which can have a stronger
58 influence on total plant productivity than the genotype alone (Voltas et al., 2002; Mohamed, 2013;
59 Solonechnyi et al., 2015; Katsenios et al., 2021; Fekadu et al., 2023). While breeding has been key for
60 crop adaptation to changing climatic factors, the rapid evolution of these factors poses significant
61 challenges. Understanding GEI is crucial to minimizing their impact in breeding programs and
62 ensuring the success of future efforts in variable and unpredictable environments.

63 Crop models are powerful tools for exploring GEI in major crops such as wheat, maize, or soybean
64 (Chenu et al., 2017; Messina et al., 2009; Schoving et al., 2020). These models can enhance our
65 understanding of the environmental regulation of plant physiology and its impact on growth and
66 development (Chapman, 2008). The strategy relies on simulating crop development in each tested
67 environment across MET, calculating a large set of environmental covariates (EC) throughout the crop
68 cycle from recorded weather data, and detecting the main GEI sources through multivariate analysis
69 (Chenu et al., 2013; Heslot et al., 2014; Rincent et al., 2019; Costa-Neto et al., 2021; Bustos-Korts et
70 al., 2022; Elmerich et al., 2023). This approach provides a detailed characterization of the
71 environments in which cultivars develop and grow. Envirotyping involves characterizing the
72 environmental conditions crops are exposed to for the definition of mega-environments, which can be
73 established based on several indicators: geographic, stress indices, variations in yield and agronomic

74 traits, or a combination of these (Chapman et al., 2000; Windhausen et al., 2012; Crespo-Herrera et al.,
75 2021; Bustos-Korts et al., 2022; Vitale et al., 2024; Corlouer et al., 2024). Envirotyping is necessary to
76 define the Target Population of Environments (TPE), focusing on mapping out the mega-
77 environments. Based on GEI-drivers, it would minimize GEI and help breeders select cultivars
78 adapted to the European environment types (ET) (Cooper and Messina, 2021). Using such
79 environmental classification, trials can be contextualized and weighted through the MET-TPE
80 alignment to better evaluate cultivar performance across the TPE (Podlich et al., 1999) and guide
81 future crosses.

82 For most crop species, cultivars are known to be either adapted to one prevalent climatic scenario (i.e.,
83 specific adaptation) or to a wide range of environments (i.e., broad adaptation). Deploying genotypes
84 that match environmental patterns detected across the TPE is essential for optimizing crop adaptation.
85 Spring crops are especially vulnerable to climate change due to their short growth cycles, which limit
86 their ability to recover from the adverse effects of increasingly frequent extreme climatic events such
87 as drought that can be counterbalanced in winter crop with a deeper root system (Olesen et al., 2011).
88 It is imperative to explore their sensitivity to climate to improve their resilience and adaptation. Spring
89 malting barley is a major spring crop, understudied in ecophysiology, widely cultivated worldwide
90 under various pedoclimatic contexts. Modern spring malting barley shows limited genetic variability,
91 making it important to identify the sources of GEI to enhance resilience against extreme climatic
92 events (Laidig et al., 2017). The main drivers of relative yield performance for spring barley genotypes
93 are not identified and prioritized. To the best of our knowledge, no envirotyping approach has been
94 dedicated to malting spring barley in Europe where specific and/or broad adaptation patterns can be
95 expected across this large production area.

96 The aim of this study is to improve our knowledge of two-row spring malting barley across the
97 European production area, specifically to (i) highlight the main environmental covariates (EC) during
98 each growth stage driving GEI for yield and (ii) characterize the nature and distribution of
99 environment types (ET) to further explore adaptation zones and genotypic performance.

101 2. Materials and method

102 2.1. Multi-environment trials

103 Grain yield from 60 two-row malting spring barley breeding lines and 52 reference cultivars grown
104 over the spring-summer season in 121 environments (location x year) from 2015 to 2022 were
105 obtained from the multi-environment trials (MET) network of SECOBRA Recherches
106 (<https://secobra.fr/en/accueil>). The trials were distributed across Northern and Western Europe,
107 including seven countries: Czech Re- public, Denmark, France, Germany, Sweden, the United
108 Kingdom (En- gland and Scotland) and Ireland (Table S1). For trials without replication information,
109 the adjusted genotype means were used. When replication data was available, adjusted means were
110 calculated by considering replication as a random effect.

111

112 2.2. Weather and soil data

113 Daily weather data, interpolated on a grid of 25 km x 25 km, were extracted from the JRS-MARS
114 Meteorological database (<https://agri4cast.jrc.ec.europa.eu/>), including minimum and maximum
115 temperatures (°C), total precipitation (mm day⁻¹), and total global ra- diation (MJ m² day⁻¹). For each
116 location, the closest weather station (< 13 km) was used. Soil parameters at each location were
117 obtained from the European Soil Database (ESDB) using a 1 km x 1 km grid
118 (<https://esdac.jrc.ec.europa.eu/>). Data extracted included clay (%), silt (%), and sand (%)
119 content, gravel content (%), bulk density (g cm⁻³), and rooting depth (cm).

120

121 2.3. Environmental covariates calculation and genotype x environment interactions analysis

122 The CERES-Barley model, part of the Decision Support System for Agrotechnology Transfer
123 (DSSAT v4.8), was calibrated to simulate the phenology of two reference cultivars (cv. RGT Planet
124 and cv. Laureate) that represented the variation in phenology among existing spring barley germplasm

125 (Table S2, Table S3) (Jones et al., 2003; Hoogenboom et al., 2019). Field experiments (nine
126 environments) were conducted in 2022 to calibrate the model for five critical growth stages: first leaf
127 through coleoptile (Z11), head at 1 cm (Z30), half of the head emerged – heading – (Z55), early milk
128 (Z73), and physiological maturity (Z90) (Zadoks et al., 1974). Cultivar coefficients were manually
129 adjusted to maximize the Willmott index of agreement (d-stat) (Willmott et al., 2012) and minimize
130 the root-mean-square error (RMSE) (Willmott et al., 1985). Model validation was performed on the
131 MET network database (see Section 2.1), where phenology data were available (38 % of the dataset),
132 providing an RMSE <4 days for heading and physiological maturity dates. The validated model was
133 then used to simulate the phenology of cv. RGT Planet and cv. Laureate in the 121 environments.
134 Daily weather data, soil properties (see Section 2.2), and management practices (sowing dates and
135 irrigation scenarios) were used as the minimum data input (Hunt and Boote, 1998). Due to the small
136 variations in simulated phenology between the two cultivars (< three days for heading and four days
137 for physiological maturity), the average simulated phenology (number of days after sowing) was used
138 to calculate a set of 138 environmental covariates (EC) – climatic variables calculated over specific
139 phenophases (growth periods between two stages in the crop cycle – in each environment. The crop
140 cycle was divided into six phenophases: Sowing to Emergence (SO-EM), Emergence to Head at 1 cm
141 (EM-1CM), Head at 1 cm to Heading (1CM-HD), Heading to Anthesis (HD-AN), Anthesis to
142 beginning Grain Filling (AN-GF), and beginning of Grain Filling to Physiological Maturity (GF-PM).
143 For each phenophase, 18 climatic variables related to daily precipitation, temperature, and solar
144 radiation were calculated. Additionally, five EC calculated by the model were considered: water stress
145 factor, top layer soil moisture, potential evapotranspiration (ETP), soil moisture, and soil temperature.
146 The water stress factor calculation was based on the maximum root water uptake to atmospheric water
147 demand ratio (Jones et al., 2003). The water stress ranges from 0 to 1, where 0 indicates no stress and
148 1 indicates maximum stress. Potential ETP was simulated using the default Priestley–Taylor method,
149 which uses net daily solar radiation and temperature (Ritchie, 1998). The model used soil and plant
150 canopy albedo to compute daily soil evaporation and plant transpiration. From the 138 EC, 91 were
151 retained for the analysis to avoid strong autocorrelations.

152 Partial Least Squares (PLS) regressions were performed to detect the most relevant EC driving
153 genotype x environment interactions (GEI) across the MET. PLS regression is a robust and commonly
154 used statistical method to predict a response variable (Y-table) from a set of explanatory variables (X-
155 matrix) in agronomy (Crossa et al., 2010). Orthogonal factors, called latent variables, with the best
156 predictive values are extracted from the X-matrix. This method is suitable when the number of
157 explanatory variables exceeds the number of observations in the Y-table and when multicollinearity is
158 observed in the X-matrix (Abdi, 2010). Another advantage of this type of analysis over linear factor
159 regression is the ability to evaluate several covariables, allowing for the integration of as many
160 environmental variables as possible, thereby limiting a priori statements about which factors to include
161 in the analysis. Variable selection methods were employed, accepting that the X-matrix can contain
162 redundant or irrelevant variables without impacting the results (Mehmood et al., 2012). A total of 15
163 PLS analyses were performed: eight single-year PLS and seven double-year PLS (Table S4). For
164 single-year analyses, only genotypes repeated across all environments of that year were used. For the
165 two-year analyses, genotypes present in all environments across both years were included in the
166 analysis (Table S4). The number of components was defined based on the Wold algorithm (Wold et
167 al., 1984, 1987, 2001; Tenenhaus et al., 2005). The Variable Importance in Projection (VIP) scores
168 were used to select variables driving GEI. Two VIP scores were calculated for each EC, based on the
169 average VIPs from the single-year PLS analyses and the double-year PLS analyses. Variables with an
170 average VIP score > 1 were considered.

171

172 *2.4. Definition of the Target Population of Environments*

173 Defining the Target Population of Environments (TPE) requires identifying, through a clustering
174 method, a set of climatic scenarios at the MET scale, called environment types (ET) to classify each
175 environ- ment (i.e., location x year) (Chapman et al., 2000; Crespo-Herrera et al., 2021; Elmerich et
176 al., 2023). To cover the European malting spring barley cropping area, 120 locations were added to the
177 initial MET database (Fig. 1). At each location, daily weather data from the period of 2013–2022, soil

178 properties extracted from the ESDB (see Section 2.2), and sowing dates were used as inputs to simulate
179 spring barley phenology for cv. RGT Planet and cv. Laureate across the 1450 environments. An
180 average phenology was used to calculate the 91 EC in each environment (see Section 2.3). For
181 environments where the sowing date was not available, the nearest date was assigned based on the
182 initial MET and national official trials.

183 Using the 35 yield GEI-drivers obtained from the method detailed in Section 2.3, combinations of 6–
184 12 EC were tested for the best clustering model. This range of parameters appears reasonable for
185 achieving a parsimonious model (Corlouer et al., 2019; Schoving et al., 2020; Elmerich et al., 2023).

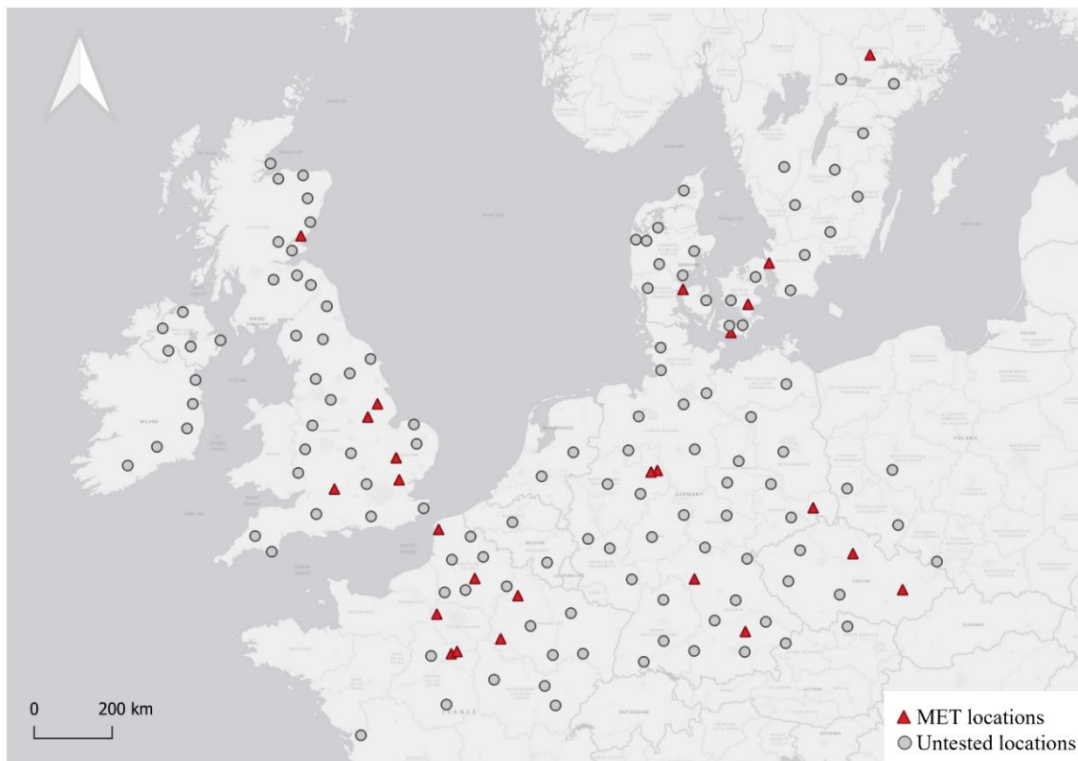
186 A hierarchical clustering was conducted based on the Euclidean distance using the hclust package (R
187 software v4.2.1) to aggregate the 35 EC into n groups, where $n \in [6; 12]$ (Ward, 1963). All
188 combinations of EC, encompassing one EC from each group, were tested, resulting in a total of 13,440
189 combinations of six EC, 26,880 of seven EC, 38,440 of eight EC, 46,080 of nine EC, 46,080 of 10 EC,
190 23,040 of 11 EC, and 15,360 of 12 EC.

191 For each combination, a K-means clustering analysis was performed on the 1450 environments using
192 the nbclust package (R software v4.2.1). The Euclidean distance and complete linkage method were
193 employed to minimize within-cluster variance and ensure that the clusters formed were well separated.
194 This process detected a set of ET encountered across the TPE for each model.

195 To choose the most parsimonious set of ET, each K-means model was fitted on observed yield data for
196 the genotypes tested at least three times in each cluster. The performance of each clustering model was
197 assessed using the method published by Elmerich et al. (2023). This method evaluates each clustering
198 model based on: (i) the significance of the genotype \times cluster interaction, which indicates variation in
199 relative performance across ET; (ii) the percentage of significant genotype \times cluster interactions
200 ($G \times C$), ensuring that the interaction involves multiple genotypes; and (iii) the ability to explain the
201 genotype \times cluster effect from the set of n EC.

202 After the envirotypes identification based on a subset of environmental covariates (ECs), a separate
203 and independent analysis was performed to finely characterize each ET. For this, the full set of 91

204 ECs was used to test the effect of each EC on the ETs using an ANOVA. A Tukey test was conducted



205 to compare the means of ET when a significant effect was observed (p -value < 0.05).

206 **Fig. 1. Distribution of the 145 selected locations used to define the Target Population of**
207 **Environments (TPE) for two-row malting spring barley across Northern and Western Europe.**
208 The red triangles represent locations tested for yield, constituting the initial Multi-Environment Trials
209 (MET). The gray dots represent untested locations for yield, added to create a continuum across the
210 geographical area of two-row malting spring barley production.

211

212

213 *2.5. Genotype plus genotype by block of environments biplot*

214 The Genotype plus Genotype by Block of Environments (GGB) biplot graphically displays genotype
215 performances and mega-environment identification in MET. It includes the two main principal
216 components (PC1 and PC2) obtained from a Principal Component Analysis on a matrix centered on
217 the environment, with genotype-by-environment data grouped by ET. The GGB biplot allows for the
218 visualization of the genotype means in each block of environments. Genotype performances can be

219 analyzed by projecting a line from the biplot origin to the marker for the ET. Genotypes can then be
 220 ordered based on their projections on the ET axis, reflecting their performance in environments
 221 representative of this ET. In this study, the ET were defined as ET-1, ET-2, and ET-3. Herein, the
 222 GGB biplot was constructed based on the 2022 PLS analysis data including grain yield evaluated for
 223 25 genotypes across 17 environments (Table S4) using the *gge* package in R software (v4.2.1)
 224 (Laffont et al., 2013).

225

226 *2.6. Evaluation of envirotypes relevance in the Target Population of Environments*

227 Two linear mixed models were used to analyze grain yield variance in the whole dataset and assess the
 228 relevance of the identified envirotypes in capturing GEL.

229 The first linear mixed model (Model 1) used as a baseline was defined as:

$$Y_{ij} = \mu + G_i + E_j + e_{ij} \text{ with } G_i \sim N(0, I\sigma^2_G), E_j \sim N(0, I\sigma^2_E) \text{ and } e_{ij} \sim N(0, I\sigma^2_e) \quad (1)$$

230 Where Y_{ij} is the observed yield for genotype i in environment j , μ is the overall mean, G_i is the random
 231 effect of genotype i , E_j is the random effect of environment j and e_{ij} is the residual error term.

232 The second linear mixed model (Model 2) extended Model 1 by incorporating a fixed envirotypes
 233 effect and a random genotypes * envirotypes effect:

$$Y_{ijk} = \mu + ET_k + G_i + E_{j(k)} + (G \times ET)_{ik} + e_{ijk} \text{ with } G_i \sim N(0, I\sigma^2_G), E_j \sim N(0, I\sigma^2_E), \\ (G \times ET)_{ik} \sim N(0, I\sigma^2_{G \times ET}) \text{ and } e_{ijk} \sim N(0, I\sigma^2_e) \quad (2)$$

234 Where Y_{ijk} is the observed yield for genotype i in environment j and envirotypes k , μ is the overall
 235 mean, ET_k is the fixed effect of envirotypes k , G_i is the same as before, $E_{j(k)}$ the random effect of
 236 environment j nested within ET k , $(G \times ET)_{ik}$ is the random interaction effect between genotype i and
 237 envirotypes k , e_{ijk} is the residual error term.

238 The variance partitioning was obtained by ReML, and the Akaike Information Criterion (AIC) was
 239 obtained using maximum likelihood.

240 **3. Results**

241

242 *3.1. Main environmental covariates explaining yield genotype x environment interactions*

243 For genotype x location interactions (*i.e.*, single-year analysis), 81% of the selected climatic variables
244 were distributed over two critical phenophases: Head at 1 cm to Heading (1CM-HD) and beginning
245 Grain Filling to Physiological Maturity (GF-PM) (Table 1). Genotype x location x year interactions
246 (*i.e.*, double-year analysis) were explained by the phenophases from 1CM to PM, with a major
247 contribution from the 1CM- HD and GF-PM phenophases, accounting for 33 % and 29 % of the
248 selected climatic variables, respectively (Table 1).

249 During the 1CM-HD phenophase, temperature-related variables, such as daily average and maximum
250 temperatures, were the most significant contributing factors to GEI. Thresholds of 15°C for average
251 temperature and 7°C and 15°C for minimum temperature impacted GEI during this phenophase.
252 Temperature also emerged as a critical variable during the GF-PM phenophase, particularly maximum
253 temperature, with the number of days exceeding 25°C and 30°C. This phenophase was also highly
254 influenced by all solar radiation variables. In both analyses, water stress and ETP during GF-PM
255 contributed to GEI. In double-year analyses, thermal amplitude emerged as the most explanatory
256 variable during the HD to GF phases.

257

258

259 **Table 1. Main environmental covariates (EC) impacting genotype x environment interactions for**
 260 **yield.** (a) Frequency of phenological stage intervals and (b) distribution of the main variables. Fifteen
 261 variables were selected after PLS regression analysis, based on their average VIP score > 1 in single-
 262 year and double-year analyses. Single-year PLS revealed EC impacting genotype x location
 263 interactions, while double-year PLS revealed EC impacting genotype x location x year interactions.
 264 The six phenological intervals were: Sowing to Emergence (SO-EM), Emergence to Head at 1 cm
 265 (EM-1CM), Head at 1 cm to Heading (1CM-HD), Heading to Anthesis (HD-AN), Anthesis to
 266 beginning Grain Filling (AN-GF), beginning Grain Filling to Physiological Maturity (GF-PM).

		Sowing (SO)	Emergence (EM)	Head 1 cm (1CM)	Heading (HD)	Anthesis (AN)	Grain Filling (GF)	Physiological Maturity (PM)
□ Genotype x Location (1 year PLS analysis)		0%	14%	38%	5%	0%	43%	
■ Genotype x Location x Year (2 years PLS analysis)		0%	0%	33%	24%	14%	29%	
DURATION	Duration			□ ■				
TEMPERATURE	Average daily temperature			□ ■	■		□	
	Thermal amplitude		□		■	■		
	Number of days below 15°C			□ ■				
MINIMUM TEMPERATURE	Average minimum temperature				■		■	
	Number of days below 7°C			□ ■				
	Number of days below 15°C			□ ■			□	
MAXIMUM TEMPERATURE	Average maximum temperature		□	□ ■	□ ■	■	□ ■	
	Number of days above 25°C			□			□	
	Number of days above 30°C						■	
RADIATION	Average daily solar radiation			□			□	
	Cumulative solar radiation						□ ■	
	Photothermal quotient		□	■	■		□	
WATER	Cumulative potential evapotranspiration						□ ■	
	Water stress factor					■	□ ■	

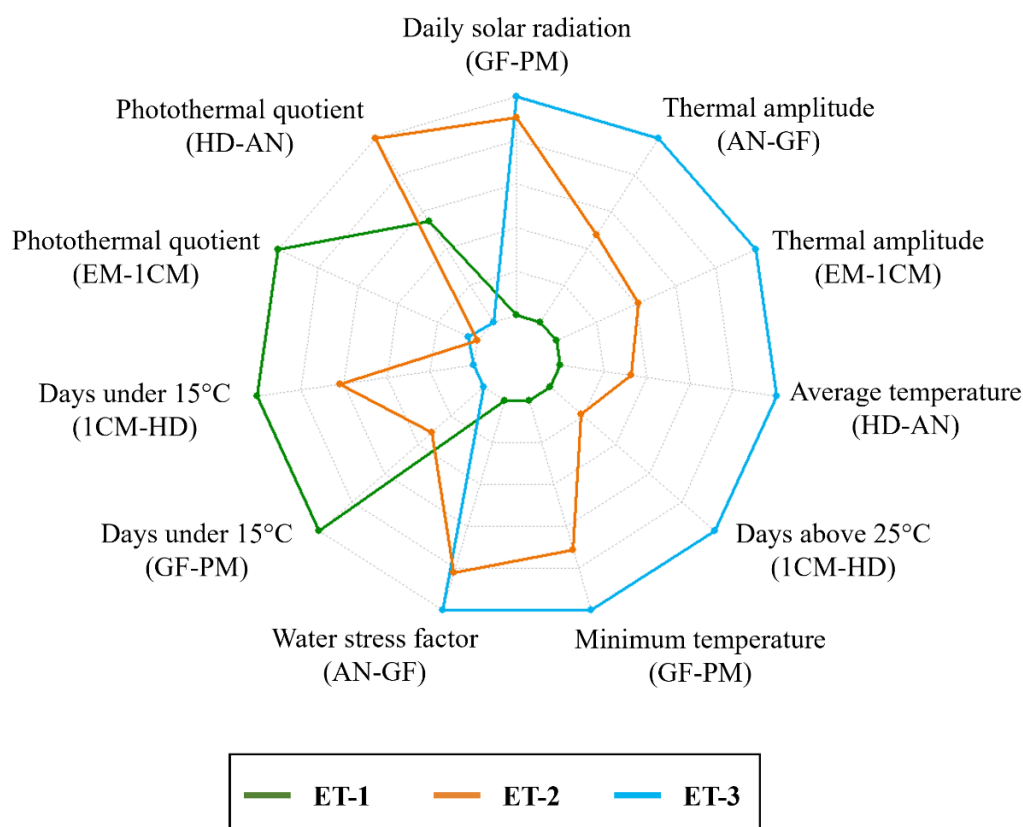
268 *3.2. Three main environment types for two-row malting spring barley in Northwestern Europe*

269 A total of 209,280 clustering models were tested on observed grain yield. Each model used a unique
270 combination of EC identified as major GEI drivers (Table 1). The best clustering model, constructed
271 using 11 EC, was selected based on the criteria detailed in Section 2.4. It was fitted on 28 genotypes.
272 In this model, 2 % of the yield variance was explained by the genotype, 2 % by the G×C effect, and
273 the combination of EC used in this clustering model explained 25 % of the G×C effect.

274 Three clusters were defined according to the thermal amplitude from Emergence to Head at 1 cm
275 (EM-1CM), the photothermal quotient during EM-1CM, the number of days above 25°C from 1CM-
276 HD, the number of days under 15°C during 1CM-HD, the photothermal quotient from Heading to
277 Anthesis (HD-AN), the average temperature from HD to AN, the thermal amplitude from Anthesis to
278 beginning Grain Filling (AN-GF), the average daily solar radiation from GF-PM, the number of days
279 under 15°C during GF-PM, the water stress factor during AN-GF, and the minimum temperature
280 during GF-PM (Fig. 2)

281 Environment types (ET) were characterized by the set of 91 EC if a significant difference was
282 observed (p -value < 0.05) (Table 2). The first envirotype (ET-1), referred to as “maritime,” was
283 characterized by the coolest temperatures throughout the crop cycle with long phenophases. No
284 thermal amplitude was observed at early stages and at anthesis (AN) (below 7°C and 8°C,
285 respectively). No heat stress was recorded from 1CM-HD and from GF-PM (number of days below
286 15°C during 1CM-HD > 24 and above 25°C during GF-PM < 3). ET-1 had the lowest solar radiation
287 levels (e.g, 16 MJ m⁻² day during GF-PM). Elevated precipitation was recorded at early stages and
288 post-AN, resulting in no water stress during EM-1CM and GF-PM (water stress factor < 0.1). The
289 second envirotype (ET-2), referred to as “temperate,” had similarities with ET-1, with cool
290 temperatures during pre-emergence and vegetative stages (number of days below 7°C during SO-EM
291 > 9). There was low thermal amplitude and no heat stress during 1CM-HD and GF-PM (number of
292 days below 15°C during 1CM-HD > 18 and above 25°C during GF-PM < 9). ET-2 differed from ET-1
293 due to elevated temperatures during GF-PM and high solar radiation levels throughout the cycle (e.g.,
294 19 MJ m⁻² day during GF-PM). Water stress was observed during EM-1CM and post-AN (water stress

295 factor > 0.4). The third envirotype (ET-3), referred to as “continental,” emerged as the most stressed
 296 environment. It had elevated temperatures from sowing to physiological maturity, resulting in short
 297 phenophases. There was high thermal amplitude during early stages and at AN (above 11°C and 12°C,
 298 respectively). Heat stress was recorded during 1CM-HD and GF-PM (number of days below 15°C
 299 during 1CM-HD < 12 and above 25°C during GF-PM > 13). This was the ET with the highest solar
 300 radiation levels throughout the cycle (e.g., 21 MJ m⁻² day during GF-PM). ET-3 had the lowest
 301 precipitation levels, resulting in water stress during the EM-1CM phenophase and post-AN stages
 302 (water stress > 0.4).



303

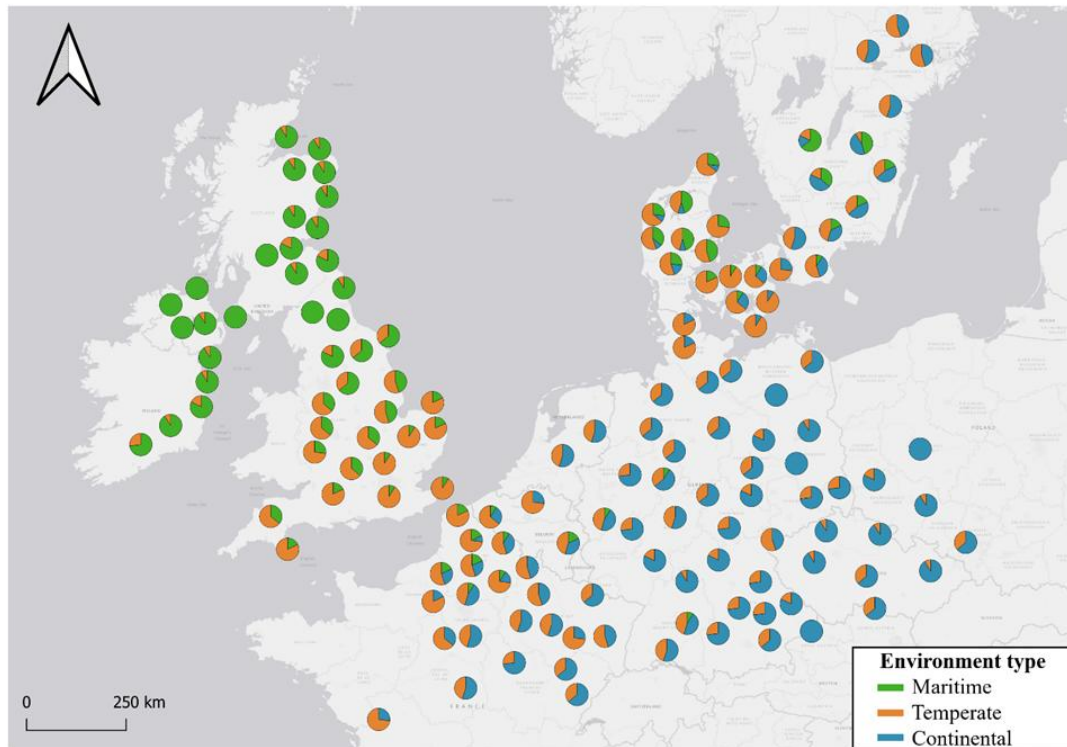
304 **Fig. 2. Characterization of the three environment types (ET) by the 11 environmental covariates**
 305 **used for clustering.** The phenophases are indicated in parentheses with the following stages: Sowing
 306 to Emergence (SO-EM), Emergence to Head at 1 cm (EM-1CM), Head at 1 cm to Heading (, 1CM-
 307 HD), Heading to Anthesis (HD-AN), Anthesis to beginning Grain Filling (AN-GF), beginning Grain
 308 Filling to Physiological Maturity (GF-PM). The inner and outer circles represent the minimum and
 309 maximum values for each eco-climatic factor, respectively. The colors indicate the envirotype: green
 310 for the first envirotype (ET-1), orange for the second envirotype (ET-2) and blue for the third
 311 envirotype (ET-3).

312 **Table 2. Description of the three environment types (ET) identified by clustering.** Yellow and blue shading correspond to the highest and lowest means of
 313 environmental covariates (EC), respectively. The EC written in bold correspond to those used for the K-means clustering.

	Variables	SOWING EMERGENCE	EMERGENCE HEAD AT 1CM	HEAD AT 1CM HEADING	HEADING ANTHESIS	ANTHESIS GRAIN FILLING	GRAIN FILLING PHYSIOLOGICAL MATURITY	Overview		
ET-1 <i>MARITIME</i>	Duration						Long phase	<i>Cool temperatures during vegetative stages, at anthesis and during grain filling. No thermal amplitude, no heat stress during stem elongation and grain filling. Low solar radiation. No water stress at emergence and grain filling.</i>		
	Temperature	min	Night temperature & TMIN < 7°C		TMIN < 7°C & TMIN < 15°C		Minimum temperature		Minimum temperature TMIN < 15°C	
		avg	Average temperature	TAVG < 15°C	TAVG < 15°C		Average temperature		Average temperature	
		max	Maximum temperature		TMAX > 25°C		Maximum temperature		Maximum temperature & TMAX > 25°C	
		ampl	Thermal amplitude	Thermal amplitude			Thermal amplitude			
	Radiation		Daily solar radiation	Daily solar radiation	Daily solar radiation	Daily solar radiation & PTQ	Daily solar radiation			
	Water	Precipitation	Water stress & ETP			Precipitation	Water stress		Water stress	
Soil	Soil temperature									
ET-2 <i>TEMPERATE</i>	Duration	Long phase						<i>Cool temperatures during vegetative stages, at anthesis but elevated during grain filling. No thermal amplitude, no heat stress during stem elongation. High solar radiation. Water stress at emergence and grain filling.</i>		
	Temperature	min	TMIN < 7°C						Minimum temperature	
		avg	Average temperature & TAVG < 7°C						Average temperature	
		max	Maximum temperature		TMAX > 25°C				Maximum temperature	
		ampl	Thermal amplitude				Thermal amplitude			
	Radiation		Daily solar radiation		PTQ	Daily solar radiation & PTQ	Daily solar radiation			
	Water	Precipitation	Water stress & ETP			Water stress & ETP	Water stress			
Soil	Soil temperature									
ET-3 <i>CONTINENTAL</i>	Duration	Short phase					Short phase	<i>Elevated temperatures during vegetative stages, at anthesis and during grain filling. Thermal amplitude, heat stress during stem elongation and grain filling. High solar radiation. High water stress at emergence and grain filling.</i>		
	Temperature	min	Night temperatures & TMIN < 7°C		TMIN < 7°C & TMIN < 15°C		Minimum temperature		Minimum temperature TMIN < 15°C	
		avg	Average temperature & TAVG < 7°C	TAVG < 15°C	TAVG < 15°C		Average temperature		Average temperature	
		max	Maximum temperature		TMAX > 25°C		Maximum temperature		Maximum temperature & TMAX > 25°C	
		ampl	Thermal amplitude	Thermal amplitude			Thermal amplitude			
	Radiation		Daily solar radiation	Daily solar radiation	Daily solar radiation	PTQ	Daily solar radiation		PTQ	Daily solar radiation
	Water	Precipitation	Water stress & ETP				Precipitation		Water stress	Water stress
Soil	Soil temperature									

316 *3.3. Definition of the European Target Population of Environments for the two-row malting spring*
317 *barley*

318 Fig. 3 displays the frequencies in time and space of ET across the European two-row malting spring
319 barley production area over the past ten years. The “continental” type (ET-3) was the most frequently
320 recorded, accounting for 40 % of the encountered climatic scenarios. The “maritime” type (ET-1) was
321 the least frequent, with a frequency of 25 %, while the “temperate” type (ET-2) appeared at 30 %. The
322 distribution of these three environmental types differed across regions. There is a gradient in the ET
323 distribution from Northwest to Southeast. In the Northwest, the “maritime” type was the most
324 recorded (i.e., Scotland and Ireland), while the “continental” type was characteristic of the Southeast
325 (i.e., Germany, Czech Republic, and Poland). Across the central geographic area, the “temperate” type
326 was the most detected. Strong repeatability of the ET occurrences was observed in Ireland and
327 Scotland, where ET-1 accounted for 90–100 % of the scenarios over the past 10 years. Some sites had
328 an equal frequency between two ETs, as in Germany, where almost all locations were either ET-2 or
329 ET-3. In contrast, low repeatability was observed in Northern France, where all ETs were recorded.
330 Despite the proximity of some places, they exhibited different patterns, as seen in central Sweden.
331 Conversely, some distant locations had similar patterns, such as between Germany and Northern
332 Sweden or between Denmark and France.



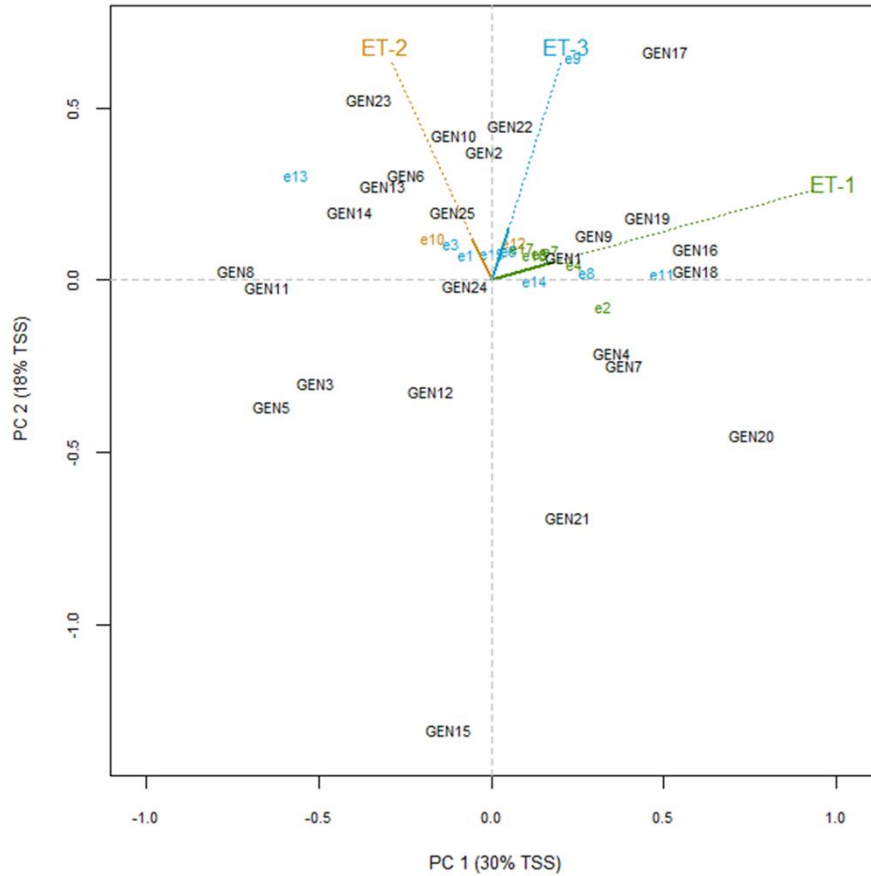
333

334 **Fig. 3. European Target Population of Environments of the two-row malting spring barley.** The
 335 environment types (ET) were defined using yield GEI-drivers. The 10- year ET frequency of
 336 occurrence was calculated and represented on the map using pie charts. The colors of each pie section
 337 indicate the envirotpe: green for the first envirotpe (ET-1), orange for the second envirotpe (ET-2),
 338 and blue for the third envirotpe (ET-3).

339

340 *3.4. Genotypic performance variation across environment types*

341 The evaluation of genotype adaptation to the three ET was achieved using a GGB biplot (Fig. 4). The
 342 MET was composed of 25 genotypes (GEN1 to GEN25) and 17 environments (e1 to e17) distributed
 343 across the three ETs: six environments were “maritime” (ET-1), two were “temperate” (ET-2), and
 344 nine were “continental” (ET-3). Some geno- types were strongly associated with a specific ET, such as
 345 GEN23, which was one of the highest-yielding genotypes in ET-2. Contrasts in perfor- mance between
 346 environments were observed for some genotypes; for example, GEN6 had good performances in ET-2
 347 while low-yielding in ET-1. GEN17 was the most high-yielding genotypes across all ET. GEN15 was
 348 the least-yielding genotypes in this MET context.



349

350 **Fig. 4. Genotype plus Genotype by Block of environments biplot illustrating the contrasted**
 351 **performances of genotypes across environment types.** The genotypes are annotated from GEN1 to
 352 GEN25 and the environments from e1 to e17. The environments are grouped into three ETs (ET-1,
 353 ET-2, and ET-3). The colors indicate the envirotypes: green for the “maritime” (ET-1), orange for the
 354 “temperate” (ET-2) and blue for the “continental” (ET-3).

355

356

357 *3.5. Evaluation of envirotypes relevance in the Target Population of Environments*

358 **Table 3. Results of the mixed linear models applied on the whole dataset to evaluate the impact**
 359 **of the envirotypes and genotypes * envirotypes effects on variance partition and Akaike**
 360 **Information Criterion.**

	<i>% variance G</i>	<i>% variance E</i>	<i>% variance GxET</i>	<i>% variance \mathcal{E}</i>	<i>AIC</i>
Model 1	1.4	91.0		7.6	15225
Model 2	2.2	89.8	1.3	6.7	15212

361

362 The whole dataset was used to estimate the variance contribution for grain yield of genotypes,
363 environments, envirotypes and genotypes * envirotypes interactions (Table 3). Two linear mixed
364 models were fitted to assess the relevance of the identified ET in capturing GEI. The first model
365 revealed that most of the variance in grain yield was attributed to environments (91 %). The
366 genotype effect accounted for 1.4 % of the total variance and 7.6 % was attributed to the
367 residual error. In the second model incorporating interaction between genotypes and
368 envirotypes, the environment effect remained dominant at 89.8 %, but the variance explained by
369 genotypes increased to 2.2 %. The GxET interaction accounted for 1.3 % and the residual error
370 was reduced to 6.7 % (Table 3). The fixed effect of envirotypes in Model 2 was not statistically
371 significant, with a p-value of 0.26. The Akaike Information Criterion (AIC) for Model 1 was
372 15225. It was slightly lower for Model 2, with a value of 15212.

373

374 4. Discussion

375 *4.1. Environmental covariates driving yield genotype x environment interactions differed from those of* 376 *yield levels*

377

378 In the European spring barley germplasm, strong genotype x envi- ronment interactions (GEI) are
379 observed despite the poor genetic di- versity (Tondelli et al., 2013). As with other spring crop species,
380 yield variation attributed to GEI often surpasses the genetic effect, requiring the identification of the
381 main yield GEI-drivers to assist breeding in crop adaptation and yield stability (Mwiinga et al., 2020;
382 Katsenios et al., 2021). GxE studies are highly dependent on both the experimental design (MET) and
383 the nature of the genetic material being studied. However, one of the main challenges in GxE analysis
384 is the limited number of repeated genotypes across environments (Table S4) (Crossa et al., 2024).
385 While our study is limited to a specific dataset, it still provides valuable insights that are reflective of
386 what can typically be observed in Western Europe. This study identified 35 environmental covariates
387 (EC) causing interactions for two-row malting spring barley across Western Europe (Table 1).
388 Interestingly, the GEI-drivers contrasted with the yield drivers (Bicard et al., 2025). Yields were

389 largely determined at early stages, while the late crop cycle was the most sensitive for interactions.
390 Our findings align with previous studies highlighting terminal heat ($T_{MAX} > 30^{\circ}\text{C}$) and drought as
391 factors affecting genotype performance during the grain filling period (Voltas et al., 1999; Hakala et
392 al., 2012; Mahalingam, 2017). In Australia, Shirdelmoghanloo et al. (2022) detected differential
393 genetic sensitivity to these factors for yield and the physical characteristics of the grain. Variability in
394 relative yield can be attributed to different stay-green potential and Radiation Use Efficiency capacity,
395 especially in shaded-prone environments (Kamal et al., 2019; Padovan et al., 2020; Shirdelmoghanloo
396 et al., 2022). The detection of potential ETP during grain filling suggests various activity levels among
397 cultivars under stress conditions, as previously observed in other species (Reynolds et al., 2002). The
398 stem elongation period was key in understanding GEI and was influenced by temperature, similar to
399 the impact on yields in some European regions (Bicard et al., 2025). Pre-heading minimum
400 temperature and thermal time have already proven to be the main GEI-drivers for yield in wheat
401 (Sanchez-Garcia et al., 2012). Elevated temperatures can lead to rapid spike growth, inadequate
402 assimilate availability, and variability in cultivar yield (Barnaba's et al., 2007; Ugarte et al., 2007).
403 While AN was poorly detected in explaining yields in Europe, it was relevant for interactions and
404 sensitive to temperature. At heading and AN, temperature proved to affect stomatal conductance,
405 transpiration, respiration, and consequently photosynthetic activity, with different responses across
406 cultivars (Hakala et al., 2012; Mahalingam and Bregitzer, 2019). Elevated temperatures can induce a
407 shorter phase, reducing nutrient capture in cultivars. The identification of GEI-drivers provides more
408 detailed knowledge of germplasm and its environmental response to guide initial breeding decisions
409 and germplasm advancement. The perspective to assist breeding programs is to unravel the genetic
410 architecture of traits involved in barley adaptation to climate (Corlouer et al., 2024). Our results
411 confirm that breeding decision-making, if based solely on yield drivers, overlooks both cultivar
412 stability and outperforming sources.

413 Our study revealed contrasted responses of genotypes despite the limited genetic pool (Tondelli et al.,
414 2013) and provides a basis for a better understanding of crop adaptation and its implications in
415 breeding. The identification of GEI-drivers demonstrated the importance of considering phenological

416 traits for the climate adaptation of crop species (Le Gouis et al., 2020; Le Roux et al., 2024). Herein,
417 AN emerged as a key period to explain long-term stability in breeding and was confirmed to be a
418 critical stage for barley's adaptation to various environments (Porker et al., 2020; Slafer and Savin,
419 2023). It is adjusted by the duration of stem elongation, which was highlighted as a major GEI-driver
420 and can be strongly manipulated through breeding (Miroslavljevic et al., 2019). Flowering-time genes
421 influence both the timing and duration of internode elongation (Huang, 2024). It has been
422 demonstrated that Ppd-h1, a photoperiod response gene regulating environmental adaptation by
423 adjusting flowering time, integrates environmental signals to modify developmental timing by
424 influencing the number of spikelets initiated on the main shoot (Gol et al., 2021). Our study revealed
425 that the relative performances of genotypes are influenced by a complexity of EC that can be used for
426 environmental classification to guide selection strategies for yield stability and barley adaptation in the
427 context of climate change.

428

429 *4.2. Envirotyping to highlight contrasting spring barley adaptation zones*

430 This first envirotyping approach in spring barley allowed for the identification of three contrasting
431 envirotypes across Europe. The latter were mainly discriminated by 11 key GEI-drivers and presented
432 distinct patterns of thermal, water, and light stress (Fig. 2). The definition of the TPE revealed
433 heterogeneities in the distribution and occurrence of the different ETs, suggesting specific and broad
434 adaptation zones (Bustos-Korts et al., 2022) (Fig. 3). In some regions, there is a predominance of one
435 specific ET over the last 10 years. Such was the case in Scotland with the “maritime” envirotpe. In
436 contrast, in other European regions such as Denmark and France, the crop was exposed to a more
437 complex pattern of climatic scenarios with low ET repeatability. Specific adaptation is characterized
438 by high-yielding cultivars in a single ET. In contrast, broad adaptation results in high performance
439 across all ETs and is stable in the TPE. One hypothesis could be the breeding history: programs based
440 in regions with low ET repeatability advanced stable genetic material, while in regions with high ET
441 repeatability, breeders designed genotypes with specific adaptations. Contrasts in ET occurrence
442 across Europe suggest adjusting the breeding strategy and exploiting existing germplasm to adapt the
443 crop to local climate conditions (Chenu et al., 2011; Elmerich et al., 2023). In regions with high

444 repeatability of one ET, developing high-yielding cultivars particularly adapted to this ET is crucial to
445 maximize yield levels. By contrast, when heterogeneity in ET distribution is observed, there is a need
446 to design cultivars with broad adaptation. Cultivars as GEN17 that suited to a multi-ET context appear
447 to be very interesting for ensuring yield stability across the European spring barley TPE, especially in
448 locations with significant year-to-year weather variation. The perspective is to design resilient
449 ideotypes adapted to the ET (Martre et al., 2015).

450 Interestingly, the definition of the TPE can be used to generate a better design of the MET for yield
451 evaluation. Our results showed that to develop material with specific adaptation for an ET such as the
452 “maritime” or “continental” type, genotypes need to be tested in the UK or in Germany. To advance
453 broadly adapted materials, yield must be assessed in regions such as Denmark or France. To achieve
454 efficient selection for both specific and broad adaptation, the MET must be a representative sample of
455 the TPE (Van Eeuwijk et al., 2016). The conventional and naive selection strategies evaluate a
456 genotype based on average performances across the trial network, and when the MET diverges from
457 the TPE, selection efficiency is reduced. MET-TPE alignment can be achieved by weighting trial
458 results based on the ET frequencies within the targeted breeding area (Podlich et al., 1999; Costa-Neto
459 et al., 2023). This method enables consistent germplasm selection aligned with the TPE, even in
460 contrasted climatic years. Breeding will thus be directed toward the TPE. The envirotypes should
461 remain stable as defined on the germplasm, but their distribution may evolve with climate change and
462 consequently influence the definition of the TPE for breeding.

463 The presence of GEI is known to reduce yield heritability and limit genetic gain highlighting the
464 importance of understanding the molecular basis of GEI and considering them in yield predictions
465 (Touzy et al., 2019; Cooper and Messina, 2021; Crossa et al., 2021; Corlouer et al., 2024). The
466 variance partition validates the efficiency of our clustering approach to capture GEI (Table 3). The
467 introduction of a GxET interaction effect indeed resulted in the reduction of the residual variance of
468 Model 1, that included GEI. Moreover, the introduction of GxET also increased the amount of genetic
469 variance, highlighting the better relevance of Model 2, confirmed by its lower AIC. The difference of
470 AIC between the two models was modest, probably because the environment effect already captured

471 around 90 % in both models. Nevertheless, the GxET interaction effect had a variance that was more
472 than half of the main genetic effect, illustrating its relative importance. Note that the fixed ET effect
473 was not significant, meaning that despite the presence of GxET interactions, the average yield was not
474 different from one ET to another. Creating homogeneous groups with similar performances would
475 increase yield heritability (Araújo et al., 2024). The ET definition offers the possibility to enhance
476 genomic selection models by optimizing the training set by ET. This will be a major step toward the
477 design of ideotypes that outperform the existing germplasm for specific or broad adaptation across the
478 TPE (Semenov et al., 2014).

479

480 5. Conclusion

481 The climatic transition necessitates adapting crops to maintain production levels. Exploring
482 genotype x environment interactions (GEI) at a large scale is a crucial step to develop high-
483 yielding and stable cultivars under a changing climate. This study investigated the GEI
484 ecophysiology of spring malting barley across Northwestern Europe using an original
485 approach that limits assumptions. Temperature during stem elongation and drought during
486 grain filling were the main GEI yield drivers. Defining the Target Population of
487 Environment (TPE) revealed three contrasting environment types (ET) that minimize GEI
488 in terms of temperature, drought, and radiation levels. Their frequency of occurrence in
489 time and space over the past 10 years showed significant heterogeneity. Evaluating the
490 performance of the existing germplasm across the TPE has improved knowledge on spring
491 crop climate adaptation by revealing malting spring barley cultivars with broad or specific
492 adaptation. Defining the TPE will guide breeding strategies to design ideotypes and help
493 breeders with cultivar positioning in the market. This method can be deployed for other
494 species and other quantitative traits, such as quality traits. For further advancement in
495 breeding, it is necessary to integrate the environmental covariates (EC) driving GEI into
496 genomic selection models to improve data predictability.

497

498

499

References

500

501 Abdi, H., 2010. Partial least squares regression and projection on latent structure regression (PLS
502 Regression). *WIREs Comp. Stat.* 2, 97–106. <https://doi.org/10.1002/wics.51>

503 Araújo, M.S., Chaves, S.F.S., Dias, L.A.S., et al., 2024. GIS-FA: an approach to integrating thematic
504 maps, factor-analytic, and envirotyping for cultivar targeting. *Theor. Appl. Genet* 137, 80.
505 <https://doi.org/10.1007/s00122-024-04579-z>

506 Barnabás, B., Jäger, K., Feher, A., 2007. The effect of drought and heat stress on reproductive
507 processes in cereals. *Plant Cell Environ.* <https://doi.org/10.1111/j.1365-3040.2007.01727.x>

508 Bicard, M., Faucon, M.-P., Pedas, P.R., Vequaud, D., Pin, P.A., Elmerich, C., Lange, B., 2025.
509 Unravelling critical climatic factors and phenological stages impacting spring barley yields across
510 Europe. *Field Crops Res.* 321, 109665. <https://doi.org/10.1016/j.fcr.2024.109665>

511 Bustos-Korts, D., Boer, M.P., Layton, J., Gehringer, A., Tang, T., Wehrens, R., Messina, C., de la
512 Vega, A.J., van Eeuwijk, F.A., 2022. Identification of environment types and adaptation zones with
513 self-organizing maps; applications to sunflower multi- environment data in Europe. *Theor. Appl.*
514 *Genet.* <https://doi.org/10.1007/s00122-022-04098-9>

515 Chapman, S.C., 2008. Use of crop models to understand genotype by environment interactions for
516 drought in real-world and simulated plant breeding trials. *Euphytica* 161, 195–208.
517 <https://doi.org/10.1007/s10681-007-9623-z>

518 Chapman, S.C., Hammer, G.L., Butler, D.G., Cooper, M., 2000. Genotype by environment
519 interactions affecting grain sorghum. III. Temporal sequences and spatial patterns in the target
520 population of environments. *Aust. J. Agric. Res.* 51, 223. <https://doi.org/10.1071/AR99022>

521 Chenu, K., Cooper, M., Hammer, G.L., Mathews, K.L., Dreccer, M.F., Chapman, S.C., 2011.
522 Environment characterization as an aid to wheat improvement: interpreting genotype–environment
523 interactions by modelling water-deficit patterns in North- Eastern Australia. *J. Exp. Bot.* 62, 1743–
524 1755. <https://doi.org/10.1093/jxb/erq459>

525 Chenu, K., Deihimfard, R., Chapman, S.C., 2013. Large-scale characterization of drought pattern: a
526 continent-wide modelling approach applied to the Australian wheatbelt – spatial and temporal trends.
527 *N. Phytol.* 198, 801–820. <https://doi.org/10.1111/nph.12192>

528 Chenu, K., Porter, J.R., Martre, P., Basso, B., Chapman, S.C., Ewert, F., Bindi, M., Asseng, S., 2017.
529 Contribution of crop models to adaptation in wheat. *Trends Plant Sci.* 22, 472–490.
530 <https://doi.org/10.1016/j.tplants.2017.02.003>

531 Cooper, Mark, Messina, Carlos D., Tang, Tom, Gho, Carla, Powell, Owen M., Podlich, Dean W.,
532 Technow, Frank, and Hammer, Graeme L. (2023). Predicting Genotype × Environment ×
533 Management (G × E × M) interactions for the design of crop improvement strategies: Integrating
534 breeder, agronomist, and farmer perspectives. *Plant breeding reviews*. Edited by Irwin Goldman.
535 Hoboken, NJ, United States: Wiley Blackwell.467-585. <https://doi.org/10.1002/9781119874157.ch8>

536 Cooper, M., Messina, C.D., 2021. Can we harness “enviromics” to accelerate crop improvement by
537 integrating breeding and agronomy? *Front. Plant Sci.* 12, 735143.
538 <https://doi.org/10.3389/fpls.2021.735143>

539 Corlouer, E., Gauffreteau, A., Bouchet, A.-S., Bissuel-B´elaygue, C., Nesi, N., Laperche, A., 2019.
540 Envirotypes based on seed yield limiting factors allow to tackle G × E interactions. *Agronomy* 9, 798.
541 <https://doi.org/10.3390/agronomy9120798>

542 Corlouer, E., Sauvage, C., Leveugle, M., Nesi, N., Laperche, A., 2024. Envirotyping within a multi-
543 environment trial allowed identifying genetic determinants of winter oilseed rape yield stability.
544 *Theor. Appl. Genet* 137, 164. <https://doi.org/10.1007/s00122-024-04664-3>

545 Costa-Neto, G., Crespo-Herrera, L., Fradgley, N., Gardner, K., Bentley, A.R., Dreisigacker, S.,
546 Fritsche-Neto, R., Montesinos-Lo´pez, O.A., Crossa, J., 2023. Envirome-wide associations enhance
547 multi-year genome-based prediction of historical wheat breeding data. *G3* 13, jkac313.
548 <https://doi.org/10.1093/g3journal/jkac313>

549 Costa-Neto, G., Crossa, J., Fritsche-Neto, R., 2021. Enviromic assembly increases accuracy and
550 reduces costs of the genomic prediction for yield plasticity in maize. *Front. Plant Sci.* 12.
551 <https://doi.org/10.3389/fpls.2021.717552>

552 Crespo-Herrera, L.A., Crossa, J., Huerta-Espino, J., Mondal, S., Velu, G., Juliana, P., Vargas, M.,
553 Pe´rez-Rodr´ıguez, P., Joshi, A.K., Braun, H.J., Singh, R.P., 2021. Target population of environments
554 for wheat breeding in india: definition, prediction and genetic gains. *Front. Plant Sci.* 12, 638520.
555 <https://doi.org/10.3389/fpls.2021.638520>

556 Crossa, J., Fritsche-Neto, R., Montesinos-Lopez, O.A., Costa-Neto, G., Dreisigacker, S., Montesinos-
557 Lopez, A., Bentley, A.R., 2021. The modern plant breeding triangle: optimizing the use of genomics,
558 phenomics, and enviromics data. *Front. Plant Sci.* 12, 651480.
559 <https://doi.org/10.3389/fpls.2021.651480>

560 Crossa, J., Montesinos-Lopez, O.A., Costa-Neto, G., Vitale, P., Martini, J.W.R., Runcie, D., Fritsche-
561 Neto, R., Montesinos-Lopez, A., Pe´rez-Rodr´ıguez, P., Gerard, G., Dreisigacker, S., Crespo-Herrera,
562 L., Pierre, C.S., Lillemo, M., Cuevas, J., Bentley, A., Ortiz, R., 2024. Machine learning algorithms
563 translate big data into predictive breeding accuracy. S1360138524002590 *Trends Plant Sci.*
564 <https://doi.org/10.1016/j.tplants.2024.09.011>

565 Crossa, J., Vargas, M., Joshi, A.K., 2010. Linear, bilinear, and linear-bilinear fixed and mixed models
566 for analyzing genotype \times environment interaction in plant breeding and agronomy. *Can. J. Plant Sci.*
567 90, 561–574. <https://doi.org/10.4141/CJPS10003>

568 Elmerich, C., Faucon, M.-P., Garcia, M., Jeanson, P., Boulch, G., Lange, B., 2023. Envirotyping to
569 control genotype \times environment interactions for efficient soybean breeding. *Field Crops Res.* 303,
570 109113. <https://doi.org/10.1016/j.fcr.2023.109113>

571 Fekadu, W., Mekbib, F., Lakew, B., et al., 2023. Genotype×environment interaction and yield stability
572 in barley (*Hordeum vulgare* L.) genotypes in the central highland of Ethiopia. *J. Crop Sci. Biotechnol.*
573 26, 119–133. <https://doi.org/10.1007/s12892-022-00166-0>

574 Gol, L., Haraldsson, E.B., von Korff, M., 2021. Ppd-H1 integrates drought stress signals to control
575 spike development and flowering time in barley. *J. Exp. Bot.* 72, 122–136.
576 <https://doi.org/10.1093/jxb/eraa261>

577 Hakala, K., Jauhiainen, L., Himanen, S.J., Ro`tter, R., Salo, T., Kahiluoto, H., 2012. Sensitivity of
578 barley varieties to weather in Finland. *J. Agric. Sci.* 150, 145–160.
579 <https://doi.org/10.1017/S0021859611000694>

580 Heslot, N., Akdemir, D., Sorrells, M.E., Jannink, J.-L., 2014. Integrating environmental covariates and
581 crop modeling into the genomic selection framework to predict genotype by environment interactions.
582 *Theor. Appl. Genet* 127, 463–480. <https://doi.org/10.1007/s00122-013-2231-5>

583 Hoogenboom, G., Porter, C.H., Boote, K.J., Shelia, V., Wilkens, P.W., Singh, U., White, J. W.,
584 Asseng, S., Lizaso, J.I., Moreno, L.P., Pavan, W., Ogoshi, R., Hunt, L.A., Tsuji, G. Y., Jones, J.W.,
585 2019. The DSSAT crop modeling ecosystem. *Burleigh Dodds Series in Agricultural Science*. Burleigh
586 Dodds Science Publishing, pp. 173–216. <https://doi.org/10.19103/AS.2019.0061.10>

587 Huang, Y., 2024. Dynamic Phytomeric Growth Contributes to Local Adaptation in Barley.
588 <https://doi.org/10.1093/molbev/msae011>

589 Hunt, L.A.,Boote, K.J. (1998) Data for Model Operation, Calibration and Evaluation. In: Tsuji, G.Y.,
590 Hoogenboom, G. and Thornton, P.K., Eds., *Understanding Options for Agricultural Production*,
591 Kluwer Academic Publishers/ICASA, Dordrecht, 9-40. https://doi.org/10.1007/978-94-017-3624-4_2

592 Intergovernmental Panel on Climate Change (IPCC) *Climate Change 2022 – Impacts, Adaptation and*
593 *Vulnerability: Working Group II Contribution to the Sixth Assessment Report of the*
594 *Intergovernmental Panel on Climate Change* 1st ed.2023 Cambridge University Press
595 <https://doi.org/10.1017/9781009325844>

596 Jones, J.W., Hoogenboom, G., Porter, C.H., Boote, K.J., Batchelor, W.D., Hunt, L.A., Wilkens, P.W.,
597 Singh, U., Gijsman, A.J., Ritchie, J.T., 2003. The DSSAT cropping system model. *Eur. J. Agron.* 18,
598 235–265. [https://doi.org/10.1016/S1161-0301\(02\)00107-7](https://doi.org/10.1016/S1161-0301(02)00107-7)

599 Kamal, N.M., Gorafi, Y.S.A., Abdelrahman, M., Abdellatef, E., Tsujimoto, H., 2019. Stay- green trait:
600 a prospective approach for yield potential, and drought and heat stress adaptation in globally important
601 cereals. *IJMS* 20, 5837. <https://doi.org/10.3390/ijms20235837>

602 Katsenios, N., Sparangis, P., Chanioti, S., Giannoglou, M., Leonidakis, D., Christopoulos, M.V.,
603 Katsaros, G., Efthimiadou, A., 2021. Genotype × environment interaction of yield and grain quality
604 traits of maize hybrids in Greece. *Agronomy* 11, 357. <https://doi.org/10.3390/agronomy11020357>

605 Laffont, J., Wright, K., Hanafi, M., 2013. Genotype plus genotype × block of environments biplots.
606 *Crop Sci.* 53, 2332–2341. <https://doi.org/10.2135/cropsci2013.03.0178>

607 Laidig, F., Piepho, H.-P., Rentel, D., Drobek, T., Meyer, U., 2017. Breeding progress, genotypic and
608 environmental variation and correlation of quality traits in malting barley in German official variety
609 trials between 1983 and 2015. *Theor. Appl. Genet* 130, 2411–2429. [https://doi.org/10.1007/s00122-](https://doi.org/10.1007/s00122-017-2967-4)
610 [017-2967-4](https://doi.org/10.1007/s00122-017-2967-4)

611 Le Gouis, J., Oury, F.-X., Charmet, G., 2020. How changes in climate and agricultural practices
612 influenced wheat production in Western Europe. *J. Cereal Sci.* 93, 102960.
613 <https://doi.org/10.1016/j.jcs.2020.102960>

614 Le Roux, R., Furusho-Percot, C., Deswarte, J.-C., Bancal, M.-O., Chenu, K., de Noblet- Ducoudr e,
615 N., de Cort azar-Atauri, I.G., Durand, A., Bulut, B., Maury, O., De come, J., Launay, M., 2024.
616 Mapping the race between crop phenology and climate risks for wheat in France under climate change.
617 *Sci. Rep.* 14, 8184. <https://doi.org/10.1038/s41598-024-58826-w>

618 Mahalingam, R., 2017. Phenotypic, physiological and malt quality analyses of US barley varieties
619 subjected to short periods of heat and drought stress. *J. Cereal Sci.* 76, 199–205.
620 <https://doi.org/10.1016/j.jcs.2017.06.007>

621 Mahalingam, R., Bregitzer, P., 2019. Impact on physiology and malting quality of barley exposed to
622 heat, drought and their combination during different growth stages under controlled environment.
623 *Physiol. Plant.* 165, 277–289. <https://doi.org/10.1111/ppl.12841>

624 Martre P., Quilot-Turion B., Luquet D., Ould-Sidi Memmah M.M., Chenu K., Debaeke P., 2015.
625 Model-Assisted Phenotyping and Ideotype Design, [https://doi.org/10.1016/B978-0-12-417104-](https://doi.org/10.1016/B978-0-12-417104-6.00014-5)
626 [6.00014-5](https://doi.org/10.1016/B978-0-12-417104-6.00014-5)

627 Mehmood, T., Liland, K.H., Snipen, L., Sæbø, S., 2012. A review of variable selection methods in
628 Partial Least Squares Regression. *Chemom. Intell. Lab. Syst.* 118, 62–69.
629 <https://doi.org/10.1016/j.chemolab.2012.07.010>

630 Messina, C., Hammer, G., Dong, Z., Podlich, D., Cooper, M., 2009. Modelling crop improvement in a
631 G×E×M framework via gene–trait–phenotype relationships. *Crop Physiol.: Appl. Genet. Improv.*
632 *Agron.* 235–265. <https://doi.org/10.1016/B978-0-12-374431-9.00010-4>

633 Miroslavljević, M., Momčilović, V., Mikić, S., Brbaklić, L., Trkulja, D., Abićić, I., 2019.
634 Changes in leaf appearance and developmental phases associated with breeding progress in six-rowed
635 barley in the Pannonian Plain. *Crop Breed. Appl. Biotechnol.* 19, 300–308.
636 <https://doi.org/10.1590/1984-70332019v19n3a42>

637 Mohamed, M., 2013. Genotype by environment interactions for grain yield in bread wheat (*Triticum*
638 *aestivum* L.). *J. Plant Breed. Crop Sci.* 7, 150–157. <https://doi.org/10.5897/JPBCS2013.0390>

639 Mwiinga, B., Sibiyi, J., Kondwakwenda, A., Musvosvi, C., Chigeza, G., 2020. Genotype x
640 environment interaction analysis of soybean (*Glycine max* (L.) Merrill) grain yield across production
641 environments in Southern Africa. *Field Crops Res.* 256, 107922.
642 <https://doi.org/10.1016/j.fcr.2020.107922>

643 Olesen, J.E., Trnka, M., Kersebaum, K.C., Skjelvåg, A.O., Seguin, B., Peltonen-Sainio, P., Rossi, F.,
644 Kozyra, J., Micale, F., 2011. Impacts and adaptation of European crop production systems to climate
645 change. *Eur. J. Agron.* 34, 96–112. <https://doi.org/10.1016/j.eja.2010.11.003>

646 Padovan, G., Martre, P., Semenov, M.A., Masoni, A., Bregaglio, S., Ventrella, D., Lorite, I. J., Santos,
647 C., Bindi, M., Ferrise, R., Dibari, C., 2020. Understanding effects of genotype \times environment \times
648 sowing window interactions for durum wheat in the Mediterranean basin. *Field Crops Res.* 259,
649 107969. <https://doi.org/10.1016/j.fcr.2020.107969>

650 Podlich, D.W., Cooper, M., Basford, K.E., Geiger, H.H., 1999. Computer simulation of a selection
651 strategy to accommodate genotype environment interactions in a wheat recurrent selection
652 programme. *Plant Breed.* 118, 17–28. <https://doi.org/10.1046/j.1439-0523.1999.118001017.x>

653 Porker, K., Coventry, S., Fettell, N., Cozzolino, D., Eglinton, J., 2020. Using a novel PLS approach for
654 envirotyping of barley phenology and adaptation. *Field Crops Res.* 246, 107697.
655 <https://doi.org/10.1016/j.fcr.2019.107697>

656 Raina, A., Laskar, R.A., Wani, M.R., Khan, S., 2022. Plant breeding strategies for abiotic stress
657 tolerance in cereals. In: Roychoudhury, A., Aftab, T., Acharya, K. (Eds.), *Omics Approach to Manage*
658 *Abiotic Stress in Cereals*. Springer Nature, Singapore, pp. 151–177. [https://doi.org/10.1007/978-981-](https://doi.org/10.1007/978-981-19-0140-9_8)
659 [19-0140-9_8](https://doi.org/10.1007/978-981-19-0140-9_8)

660 Reynolds, M.P., Trethowan, R., Crossa, J., Vargas, M., Sayre, K.D., 2002. Physiological factors
661 associated with genotype by environment interaction in wheat. *Field Crops Res.* 75, 139–160.
662 [https://doi.org/10.1016/S0378-4290\(02\)00023-0](https://doi.org/10.1016/S0378-4290(02)00023-0)

663 Rincent, R., Malosetti, M., Ababaei, B., Touzy, G., Mini, A., Bogard, M., Martre, P., Le Gouis, J., van
664 Eeuwijk, F., 2019. Using crop growth model stress covariates and AMMI decomposition to better
665 predict genotype-by-environment interactions *Theor. Appl. Genet* 132, 3399–3411.
666 <https://doi.org/10.1007/s00122-019-03432-y>

667 Ritchie, J.T., 1998. Soil water balance and plant water stress. In: Tsuji, G.Y., Hoogenboom, G.,
668 Thornton, P.K. (Eds.), *Understanding Options for Agricultural Production, Systems Approaches for*
669 *Sustainable Agricultural Development*. Springer Netherlands, Dordrecht, pp. 41–54.
670 https://doi.org/10.1007/978-94-017-3624-4_3

671 Sanchez-Garcia, M., A lvaro, F., Mart n-S´anchez, J.A., Sillero, J.C., Escribano, J., Royo, C., 2012.
672 Breeding effects on the genotype×environment interaction for yield of bread wheat grown in Spain
673 during the 20th century. *Field Crops Res.* 126, 79–86. <https://doi.org/10.1016/j.fcr.2011.10.001>

674 Schoving, C., Sto ckle, C.O., Colombet, C., Champolivier, L., Debaeke, P., Maury, P., 2020.
675 Combining simple phenotyping and photothermal algorithm for the prediction of soybean phenology:
676 application to a range of common cultivars grown in Europe. *Front. Plant Sci.* 10, 1755.
677 <https://doi.org/10.3389/fpls.2019.01755>

678 Semenov, M.A., Stratonovitch, P., Alghabari, F., Gooding, M.J., 2014. Adapting wheat in Europe for
679 climate change. *J. Cereal Sci.* 59, 245–256. <https://doi.org/10.1016/j.jcs.2014.01.006>

680 Shirdelmoghanloo, H., Chen, K., Paynter, B.H., Angessa, T.T., Westcott, S., Khan, H.A., Hill, C.B.,
681 Li, C., 2022. Grain-filling rate improves physical grain quality in barley under heat stress conditions
682 during the grain-filling period. *Front. Plant Sci.* 13. <https://doi.org/10.3389/fpls.2022.858652>

683 Slafer, G.A., Savin, R., 2023. Comparative performance of barley and wheat across a wide range of
684 yielding conditions. Does barley outyield wheat consistently in low- yielding conditions? *Eur. J.*
685 *Agron.* 143, 126689. <https://doi.org/10.1016/j.eja.2022.126689>

686 Snowdon, R.J., 2021. Crop adaptation to climate change as a consequence of long-term breeding.
687 *Theor. Appl. Genet.* <https://doi.org/10.1007/s00122-020-03729-3>

688 Solonechnyi, P., Vasko, N., Naumov, A., Solonechnaya, O., Vazhenina, O., Bondareva, O.,
689 Logvinenko, Y., 2015. GGE biplot analysis of genotype by environment interaction of spring barley
690 varieties. *Zemdirb. Agric.* 102, 431–436. <https://doi.org/10.13080/z- a.2015.102.055>

691 Tenenhaus, M., Vinzi, V.E., Chatelin, Y.-M., Lauro, C., 2005. PLS path modeling. *Comput. Stat. Data*
692 *Anal.* 48, 159–205. <https://doi.org/10.1016/j.csda.2004.03.005>. Tondelli, A., Xu, X., Moragues, M.,
693 Sharma, R., Schnaithmann, F., Ingvarlsen, C., Manninen, O., Comadran, J., Russell, J., Waugh, R.,
694 Schulman, A.H., Pillen, K., Rasmussen, S.K., Kilian, B., Cattivelli, L., Thomas, W.T.B., Flavell, A.J.,
695 2013. Structural and temporal variation in genetic diversity of European spring two-row barley

696 cultivars and association mapping of quantitative traits. *Plant Genome* 6, plantgenome2013.03.0007.
697 <https://doi.org/10.3835/plantgenome2013.03.0007>

698 Touzy, G., Rincet, R., Bogard, M., Lafarge, S., Dubreuil, P., Mini, A., Deswarte, J.-C., Beauchêne,
699 K., Le Gouis, J., Praud, S., 2019. Using environmental clustering to identify specific drought tolerance
700 QTLs in bread wheat (*T. aestivum* L.). *Theor. Appl. Genet* 132, 2859–2880.
701 <https://doi.org/10.1007/s00122-019-03393-2>

702 Trnka, M., Rötter, R.P., Ruiz-Ramos, M., Kersebaum, K.C., Olesen, J.E., Zalud, Z., Semenov, M.A.,
703 2014. Adverse weather conditions for European wheat production will become more frequent with
704 climate change. *Nat. Clim. Change* 4, 637–643. <https://doi.org/10.1038/nclimate2242>

705 Ugarte, C., Calderini, D.F., Slafer, G.A., 2007. Grain weight and grain number responsiveness to pre-
706 anthesis temperature in wheat, barley and triticale. *Field Crops Res.* 100, 240–248.
707 <https://doi.org/10.1016/j.fcr.2006.07.010>

708 Van Eeuwijk, F.A., Bustos-Korts, D.V., Malosetti, M., 2016. What should students in plant breeding
709 know about the statistical aspects of genotype × environment interactions? *Crop Sci.* 56 (5), 2119–
710 2140. <https://doi.org/10.2135/cropsci2015.06.0375>

711 Vitale, P., Crossa, J., Vaccino, P., De Vita, P., 2024. Defining the target population of environments
712 for wheat (*Triticum aestivum* L.) breeding in Italy based on historical. *Plant Breed.*
713 <https://doi.org/10.1111/pbr.13192>

714 Vogel, E., Donat, M.G., Alexander, L.V., Meinshausen, M., Ray, D.K., Karoly, D., Meinshausen, N.,
715 Frieler, K., 2019. The effects of climate extremes on global agricultural yields. *Environ. Res. Lett.* 14,
716 054010. <https://doi.org/10.1088/1748-9326/ab154b>

717 Voltas, J., Eeuwijk, F., Igartua, E., Moral, del, Molina-Cano, J., Romagosa, I., 2002. Genotype by
718 environment interaction and adaptation in barley breeding: basic concepts and methods of analysis.
719 *Barley Sci. Recent Adv. Mol. Biol. Agron. yield Qual.* [https://doi.org/10.1007/978-1-4614-5797-](https://doi.org/10.1007/978-1-4614-5797-8_199)
720 [8_199](https://doi.org/10.1007/978-1-4614-5797-8_199)

721 Voltas, J., van Eeuwijk, F.A., Sombrero, A., Lafarga, A., Igartua, E., Romagosa, I., 1999. Integrating
722 statistical and ecophysiological analyses of genotype by environment interaction for grain filling of
723 barley I. Individ. grain Weight. *Field Crops Res.* [https://doi.org/10.1016/S0378-4290\(99\)00006-4](https://doi.org/10.1016/S0378-4290(99)00006-4)

724 Ward, J.H., 1963. Hierarchical grouping to optimize an objective function. *J. Am. Stat. Assoc.* 58
725 (301), 236–244. <https://doi.org/10.1080/01621459.1963.10500845>

726 Webber, H., Ewert, F., Olesen, J.E., Müller, C., Fronzek, S., Ruane, A.C., Bourgault, M., Martre, P.,
727 Ababaei, B., Bindi, M., Ferrise, R., Finger, R., Fodor, N., Gabaldo'n- Leal, C., Gaiser, T., Jabloun, M.,
728 Kersebaum, K.-C., Lizaso, J.I., Lorite, I.J., Manceau, L., Moriondo, M., Nendel, C., Rodríguez, A.,
729 Ruiz-Ramos, M., Semenov, M. A., Siebert, S., Stella, T., Stratonovitch, P., Trombi, G., Wallach, D.,
730 2018. Diverging importance of drought stress for maize and winter wheat in Europe. *Nat. Commun.* 9,
731 4249. <https://doi.org/10.1038/s41467-018-06525-2>

732 Willmott, C.J., Ackleson, S.G., Davis, R.E., Feddema, J.J., Klink, K.M., Legates, D.R., O'Donnell, J.,
733 Rowe, C.M., 1985. Statistics for the evaluation and comparison of models. *J. Geophys. Res.: Oceans*
734 90, 8995–9005. <https://doi.org/10.1029/JC090iC05p08995>

735 Willmott, C.J., Robeson, S.M., Matsuura, K., 2012. A refined index of model performance. *Int. J.*
736 *Climatol.* 32, 2088–2094. <https://doi.org/10.1002/joc.2419>

737 Windhausen, V.S., Wagener, S., Magorokosho, C., Makumbi, D., Vivek, B., Piepho, H.-P.,
738 Melchinger, A.E., Atlin, G.N., 2012. Strategies to subdivide a target population of environments:
739 results from the CIMMYT-led maize hybrid testing programs in Africa. *Crop Sci.* 52, 2143–2152.
740 <https://doi.org/10.2135/cropsci2012.02.0125>

741 Wold, S., Geladi, P., Esbensen, K., O'hman, J., 1987. Multi-way principal components-and PLS-
742 analysis. *J. Chemom.* 1, 41–56. <https://doi.org/10.1002/cem.1180010107>

743 Wold, S., Ruhe, A., Wold, H., 1984. The collinearity problem in linear regression: the partial least
744 squares (PLS) approach to generalized inverse. *SIAM J. Sci. Stat. Comput.* 5 (3), 735–743.
745 <https://doi.org/10.1137/0905052>

746 Wold, S., Sjöström, M., Eriksson, L., 2001. PLS-regression: a basic tool of chemometrics. *Chemom.*
747 *Intell. Lab. Syst.* 58, 109–130. [https://doi.org/10.1016/S0169-7439\(01\)00155-1](https://doi.org/10.1016/S0169-7439(01)00155-1)

748 Xie, W., Xiong, W., Pan, J., Ali, T., Cui, Q., Guan, D., Meng, J., Mueller, N.D., Lin, E., Davis, S.J.,
749 2018. Decreases in global beer supply due to extreme drought and heat. *Nat. Plants* 4, 964–973.
750 <https://doi.org/10.1038/s41477-018-0263-1>

751 Zadoks, J.C., Chang, T.T., Konzak, C.F., 1974. A decimal code for the growth stages of cereals. *Weed*
752 *Res.* 14, 415–421. <https://doi.org/10.1111/j.1365-3180.1974.tb01084.x>

753

754

Funding

755 This research did not receive any specific grant from funding agencies in the public, commercial, or
756 not-for-profit sectors.

757

CRedit authorship contribution statement

758 **Bicard Maëva:** Writing – review & editing, Writing – original draft, Methodology, Investigation,
759 Formal analysis, Conceptualization. **Lange Bastien:** Writing – review & editing, Writing – original
760 draft, Methodology, Formal analysis, Conceptualization. **Elmerich Chloé:** Writing – review &
761 editing, Writing – original draft, Methodology, Formal analysis. **Pin Pierre:** Writing – review &
762 editing, Writing – original draft, Resources, Methodology, Conceptualization. **Vequaud Dominique:**
763 Writing – review & editing, Writing – original draft, Methodology, Conceptualization. **Dockter**
764 **Christoph:** Writing – review & editing, Writing – original draft, Resources, Methodology,
765 Conceptualization. **Faucon Michel-Pierre:** Writing – review & editing, Writing – original draft,
766 Methodology, Conceptualization. **Renaud Rincent:** Methodology, Formal analysis, Writing - Review
767 & Editing.

768

Declaration of Competing Interest

769 The authors declare that they have no known competing financial interests or personal relationships
770 that could have appeared to influence the work reported in this paper.

771

Acknowledgments

772 The authors are grateful to Dr. Martin Toft Simmelsgaard Nielsen, Salim Trouchaud, Sabine Bous,
773 Paul Bury and Damien Follet, the spring barley breeders of the Carlsberg Research Laboratory and
774 SECOBRA, for monitoring trials and collecting data during the crop model calibration process. The
775 authors are thankful to Gu´enol´e Boulch for its contribution to the project’s initiative and its advice.
776 We are grateful to Dr. Tony Hunt for his help in the crop model calibration. We are grateful to Dr.

777 Nicolas Honvault for his advice on statistical analysis. We acknowledge Dr. Jacques Le Gouis, Dr.
778 Vincent Allard and Dr. Thierry Aussenac for their recommendations.

779 Appendix A. Supporting information

780 Supplementary data associated with this article can be found in the online version at
781 doi:10.1016/j.fcr.2025.109793.

782 Data availability

783 The data that has been used is confidential.